The long non-coding RNA *Pax6os1*/*PAX6-AS1* modulates pancreatic β-cell identity and function.

Livia Lopez-Noriega[1]*, Rebecca Callingham[1]*, Aida Martinez-Sánchez[1], Grazia Pizza[1], Nejc Haberman[2], Nevena Cvetesic[2], Boris Lenhard[2], Piero Marchetti[3], Lorenzo Piemonti[4,5], Eelco de Koning[6,7], A. M. James Shapiro[8], Paul R. Johnson[9], Isabelle Leclerc[1], Timothy J. Pullen[1,10]†, and Guy A. Rutter[1,11]†

[1] Department of Medicine, Section of Cell Biology and Functional Genomics, Imperial College London, London, UK

[2] MRC London Institute of Medical Sciences, London, UK

[3] Department of Clinical and Experimental Medicine, University of Pisa, Pisa

[4] San Raffaele Diabetes Research Institute (SR–DRI), Istituto di Ricovero e Cura a Carattere Scientifico (IRCCS) San Raffaele Scientific Institute, Milan, Italy

[5] Vita-Salute San Raffaele University, Milan, Italy

[6]Department of Medicine, Leiden University Medical Center, Leiden, The Netherlands

[7]Hubrecht Institute, Utrecht, The Netherlands

[8] Clinical Islet Laboratory and Clinical Islet Transplant Program, University of Alberta, Edmonton, Alberta, Canada

[9] Nuffield Department of Surgical Sciences, University of Oxford, Oxford, United Kingdom

[10] Department of Diabetes, King's College London, London, UK

[11] Lee Kong Chian School of Medicine, Nanyang Technological University, Singapore

***Equal contributions**

†Correspondence to Guy. A Rutter, g.rutter@imperial.ac.uk and Timothy J. Pullen, timothy.pullen@kcl.ac.uk

Key words: Long non-coding RNAs, Pax6os1/PAX6-AS1, pancreatic β-cell, Type 2 Diabetes.

Abbreviations:

EDU 5-ethynyl-2'-deoxyuridine

GSIS glucose-stimulated insulin secretion;

HbA1c glycated haemoglobin

IPGTT intraperitoneal glucose tolerance test

HFD high fat diet

KO Knockout

LncRNA Long non-coding RNA

MTT 3-(4,5-Dimethylthiazol-2-yl)-2,5-diphenyltetrazolium bromide

RNASeq Massive parallel RNASequencing

siRNA small interfering RNA

STD Standard diet

T2D Type 2 Diabetes

Abstract

Long non-coding RNAs (lncRNAs) are emerging as crucial regulators of β-cell development and function. Consequently, the mis-expression of members of this group may contribute to the risk of type 2 diabetes (T2D). Here, we investigate roles for an antisense lncRNA expressed from the Pax6 *locus* (annotated as *Pax6os1* in mice and *PAX6-AS1* in humans) in β-cell function. The transcription factor *Pax6* is required for the development of pancreatic islets and maintenance of a fully differentiated β-cell phenotype. *Pax6os1/PAX6-AS1* expression was increased in pancreatic islets and β-cell lines at high glucose concentrations, in islets from mice fed a high fat diet, and in those from patients with type 2 diabetes. Silencing or deletion of *Pax6os1*/*PAX6-AS1* in MIN6 cells and EndoC-βH1cells, respectively, upregulated β-cell signature genes, including insulin. Moreover, shRNA-mediated silencing of *PAX6-AS1* in human islets not only increased insulin mRNA, but also enhanced glucose-stimulated insulin secretion and calcium dynamics. In contrast, inactivation of *Pax6os1* in mice was largely without effect on glucose homeostasis, though female *Pax6os1* null mice on high fat diet (HFD) showed a tendency towards enhanced glucose clearance. Together, our results suggest that increased expression of *PAX6-AS1* at high glucose levels may contribute to β-cell dedifferentiation and failure in some forms of type 2 diabetes. Thus, targeting *PAX6-AS1* may provide a promising strategy to enhance insulin secretion and improve glucose homeostasis in type 2 diabetes.

.

Introduction

Type 2 Diabetes (T2D) usually develops when β-cells within the pancreatic islet no longer secrete sufficient insulin to overcome insulin resistance and lower circulating blood glucose levels. This can promote a vicious circle leading to further β-cell failure, more severe hyperglycaemia and ensuing disease complications[1]. In a subset of patients, defective insulin secretion is observed despite near-normal insulin sensitivity[2], while in all forms of the disease, changes in β-cell "identity" are thought to play an important role in functional impairment and the selective loss of glucose responsiveness[3]. A deeper understanding of the mechanisms that influence these changes is therefore likely to facilitate the discovery of new treatments[4].

Loss of normal β-cell function is often characterized by decreased expression of insulin (*INS*) as well as of genes critical for glucose entry (the glucose transporters GLUT1/*SLC2A1*, GLUT2/*SLC2A2*) and metabolism (Glucokinase, *GCK*)[5 3]. These changes may be accompanied by increased expression of so-called "disallowed genes", whose levels are unusually low in healthy β- compared to other cell types[6]. In several models of diabetes, the above changes are associated with decreased expression of transcription factors that are required to maintain a mature β-cell phenotype, including pancreatic duodenum homeobox-1 (*PDX1*) [7] and MAF BZIP Transcription Factor A (*MAFA*)[8].

The transcription factor *Pax6* regulates the expression of several genes involved in insulin processing (prohormone convertase 1/3) and secretion (Glucagon-like peptide-1 receptor, *Glp1r*), while repressing signature genes defining different endocrine cell lineages, such as ghrelin (*Ghrl*) [9-11]. As a result, *Pax6* expression is key to maintaining β-cell identity and function. Remarkably, embryonic deletion of *Pax6* in the murine pancreas leads to a drastic reduction in the number of α- and β-cells, resulting in the death of mutant mice at postnatal days 3-6 due to severe hyperglycaemia[12]. Furthermore, conditional inactivation of *Pax6* in adult mice leads to impaired β-cell function and glucose intolerance[12,13], demonstrating its continued importance in the mature β-cell. Moreover, *Pax6* levels are reduced in pancreatic islets from Zucker diabetic fatty (ZDF)[14] rats as well as in pregnant rats fed with high fat diet[15] and, in humans, loss-of-function mutations in *PAX6* are associated with aniridia (iris hypoplasia) and T2D[16,17]. In addition, decreased *PAX6* expression in human pancreatic islets correlates with impaired insulin secretion and increased glycated haemoglobin (HbA1c)[18]. Thus, a better understanding

of how *PAX6* expression is regulated may provide useful insights into the mechanisms involved in T2D pathogenesis.

Long non-coding RNAs (lncRNAs), defined as transcripts > 200 nucleotides in length that are not translated into proteins, are crucial components of the pancreatic islet regulome, whose mis-expression may also contribute to the development of T2D [19]. Importantly, lncRNAs are expressed in a highly cell-type specific manner, making them well placed to be involved in cell lineage specification. More than 1,100 lncRNAs have been identified in both human and murine pancreatic islets. Furthermore, the expression of several of these is modulated by high glucose concentrations, suggesting that they may be involved in β-cell compensation in response to high insulin demand[20]. Interestingly, a number of β-cell-enriched lncRNAs are mapped to genetic loci in the proximity of β-cell signature genes, such as *PDX1*, and regulate their expression in *cis*[20,21].

In the current study, we sought to determine whether a lncRNA expressed from the *PAX6* locus, previously annotated as *Pax6 opposite strand 1* (*Pax6os1*) in mice and *PAX6 antisense 1* (*PAX6-AS1*) in humans[22], might impact β-cell identity and/or function through the modulation of *Pax6* expression or by other mechanisms. We show that *Pax6os1* expression is enriched in islets and, more specifically, in β-cells. Furthermore, *Pax6os1*/*PAX6-AS1* expression was upregulated in pancreatic islets from mice challenged with high fat diet (HFD) as well as in human islets from type 2 diabetic donors. Importantly, we also show that silencing or inactivation of *Pax6os1* and *PAX6-AS1* in mouse and human β-cells, respectively, upregulates several β-cell signature genes and enhances insulin production.

Materials and Methods

Animals

All animal procedures were performed with approval from the British Home Office under the UK Animal (Scientific Procedures) Act 1986 (Project License PPL PA03F7F07 to I.L.) and from the local ethical committee (Animal Welfare and Ethics Review Board, AWERB), at the Central Biological Services (CBS) unit at the Hammersmith Campus of Imperial College London and the EU Directive 2010/63/EU for animal experiments. Animals were housed in individually ventilated cages (one to five mice per cage) and kept under controlled environmental conditions (12 hs-light–dark cycle, 23 ± 1 °C with 30–50% relative humidity). Mice were provided with standard rodent chow, unless stated otherwise, and sterilized tap water *ad libitum.* For the HFD study, a chow enriched with 58% Fat and 25% Sucrose diet (D12331, Research Diet, New Brunswick, NJ) was used.

Metabolic tests

For intraperitoneal glucose tolerance tests (IPGTT), animals were fasted for 16 h prior to experiments and received an intraperitoneal injection of glucose (1 g/kg of body weight). Blood glucose levels were determined by tail venepuncture using a glucose meter (Accuchek; Roche, Burgess Hill, U) at 0, 15, 30, 60 and 120 min. after the glucose load. For insulin measurements mice received a glucose injection of 3g/kg of body weight and blood was collected in EDTA covered tubes at times 0, 15 and 30 min. after the glucose load. Subsequently, blood was centrifuged at 4000 x g during 20 min. at 4 ºC and plasma was collected. Insulin was determined by ELISA (CrystalChem, 90080), according to the manufacturer's instructions.

Human islets

Human islets were cultured in RPMI-1640 (11879-020) supplemented with 5.5 mM glucose, 10% FBS, 1% penicillin/streptomycin and 0.25 μg/ml fungizone. The characteristics of the donors and isolation centres used for this study are outlined in Supplemental Table 1.

Small interfering RNA *Pax6os1* in MIN6

MIN6 cells were transfected with a pool of three small interfering RNAs (siRNAs) targeting *Pax6os1* or three control siRNAs (table 2) using Lipofectamine™ RNAiMAX, according to the manufacturer's protocol.

Generation of *Pax6os1*-null mice.

A *Pax6os1* null mouse line was generated using a CRISPR-Cas9 strategy. Guides targeting Pax6os1 for Cas9-mediated CRISPR disruption were identified using online design software at http://crispr.mit.edu. The two targeting sequences were designed to delete ~720 bp including exon 1 of Pax6os1 and upstream region (Table 2). DNA oligos were synthesized by Sigma and the overlapping PCR products were cloned into a pX330-U6-Chimeric_BB-CBh-hSpCas9 plasmid (Addgene). Guide RNAs were validated in vitro in MIN6 cells and the deletion was confirmed via extraction of genomic DNA from an unselected pool of cells and PCR amplification using primers spanning a 930 bp region, encompassing the targeted region.

Following confirmation that the CRISPR-Cas9 had successfully produced the desired deletion, pronuclear injection of the two chosen gRNAs was performed by the MRC transgenics unit, Imperial College London. F0 compound homozygous males (carrying different mutations in the *Pax6os1* gene) were crossed with WT females. F1 heterozygous mice were sequenced to determine which mutation they were harbouring. Heterozygous mice positive for the same mutation were then crossed to generate wild-type, heterozygous and homozygous littermates.

CRISPR-Cas9 gene editing in humans and lentivirus production

Guide RNAs targeting PAX6-AS1 gene for Cas9-mediated CRISPR disruption were designed using http://crispr.mit.edu in order to delete ~80 base pairs within exon 1 of the gene. Guide RNAs were then cloned into a LentiCRISPRv2 vector (Addgene #52961) modified to replace the CMV for the rat insulin promoter (RIP) and kindly provided by Dr Paul Gadue for studies performed in human cells. Lentiviral particles were generated by co-transfection of lentiviral vectors as above together with packaging (psPAX2; Addgene, # 12260) and envelope (pMD2.G; Addgene, #12259) plasmids into HEK293T cells at 70-80% confluency using calcium phosphate. Viral supernatants were harvested 48- and 72-h post-transfection, filtered using a 0.45 μm Millex-HV filter, and concentrated by 20% sucrose gradient ultracentrifugation in an Optima XPN-100 ultracentrifuge at 26,000 rpm at 4ºC for 2 h in a SW32 Ti swinging bucket rotor (Beckman-Coulter). Viral particles were resuspended in PBS and stored at -80ºC.

Transduction of pancreatic islets

Human islets were incubated with 1.0 mL of warm (37 ºC) 0.5 X trypsin-EDTA (250 mg/L trypsin; 0.48 mM EDTA) for 3 min. in a cell culture incubator (37 ºC, 5% CO2). Trypsin activity was subsequently inhibited by adding 1.0 mL of RPMI complete medium and islets were centrifuged at 50 x g for 2 min. Afterwards, the supernatant was removed and islets were resuspended in serum free RPMI. Lentiviruses were added at multiplicity of infection (MOI) 20, assuming that a single islet has 1000 cells. Pancreatic islets were incubated over-night in a cell culture incubator (37 ºC, 5% CO2) and the medium was changed to complete RPMI[23]. For optimal lentiviral transduction and islet viability, experiments were carried out at 48 h post-infection.

Massive parallel RNASequencing (RNASeq)

MIN6 cells were harvested 72 hours post-transfection with siRNA and RNA extracted using Trizol. Islets were isolated from six wild-type and six homozygous *Pax6os1* null female mice and RNA extracted with Trizol. In both cases, RNA was DNase treated with TURBO DNase (Invitrogen) in accordance with the manufacturer's instructions. The quantity and integrity of the RNA was assessed with the RNA 6000 Nano Kit (Agilent) and an Agilent 2100 Bioanalyzer. A total of 500 ng mRNA was enriched using a NEBNext Poly(A) mRNA Magnetic Isolation Kit (NEB). Double stranded cDNA libraries were constructed using a NEBNext Ultra II Directional RNA Library Prep Kit for Illumina (NEB) and NeBNext Multiplex Adapters (NEB) used for adapter ligation. Size selection of libraries was performed with SPRIselect Beads (Beckman Coulter). The Adaptor ligated DNA was PCR amplified using NEBNext Ultra II Q5 Master Mix and Universal i5 and i7 primers provided in the NEBNext Kits.

The Imperial BRC Genomics Facility performed sequencing as 75 bp paired end reads on a HiSeq4000 according to Illumina specifications. An average of 37.7 million reads per sample were mapped to mouse genome (GRCm38) using HiSat2 and quantified using featureCounts and Ensembl annotations (v92). Differential expression analysis was performed with DESeq2 using an adjusted p-value threshold of <0.1[24-26]. Gene Set Enrichment Analysis (GSEA) was performed using the *fgsea* package with MSigDB gene sets provided by the *msigdbr* package.

Glucose-stimulated insulin secretion (GSIS)

Control and *PAX6-AS1*-depleted cells were incubated overnight in DMEM medium (Gibco, 11966025) supplemented with 3 mM glucose, 2% (w/v) albumin from bovine serum fraction V (BSA), 50 μM 2-mercaptoethanol, 10 mM nicotinamide (VWR), 5.5 μg/ml transferrin (Sigma-Aldrich), 6.7 ng/ml sodium selenite (Sigma-Aldrich) and 1% penicillin/streptomycin. After 16 h of fasting, cells were incubated with KRBH buffer (460 mM NaCl, 20 mM KCl, 4 mM CaCl2, 4 mM $MgCl_2$, 96 mM $NaHCO_3$ and 0.2% BSA, saturated with 95% O_2/5% CO_2; pH 7.4) supplemented with 0.5 mM glucose for 1 h. Afterwards, cells were incubated with either 0.5 or 15 mM glucose for another h. Supernatant was centrifuged at 3000 rpm for 5 min. at 4ºC and stored at -20ºC. Cells were lysed for total insulin content with 1M Tris pH 8.0, 1% Triton, 10% glycerol, 5M NaCl and 0.2 EGTA.

Human islets were pre-incubated in Krebs-Ringer bicarbonate-HEPES buffer (KRBH) (140 mM NaCl, 3.6 mM KCl, 0.5 mM NaH_2PO_4, 0.5 mM $MgSO_4$, 1.5 mM $CaCl_2$, 2 mM $NaHCO_3$, 10 mM HEPES, 0.1 % (w/v) BSA supplemented with 3 mM of glucose for 1 h a cell culture incubator (37 ºC, 5% CO_2). Groups of 15 islets were then transferred to Eppendorf tubes and incubated for 30 min. in fresh KRBH buffer at 37 ºC under rotation in a water bath. Islets were then centrifuged at 50 x g for 2 min. and the supernatant was stored in a new tube (basal insulin secretion). Afterwards, 500 ul of KRBH supplemented with 17 mM glucose were added. Islets were incubated for an additional 30 min. prior being centrifuged and supernatant stored (glucose-stimulated insulin secretion) [27]. Total insulin was extracted by adding acidified ethanol (75% ethanol/1.5% HCl). Insulin was measured by using a Homogeneous Time Resolved Fluorescence (HTRF) insulin assay kit (Cisbio) in a PHERAstar reader (BMG Labtech), following the manufacturer's instructions.

Immunofluorescence

Cells were fixed with 100% methanol at -20 ºC and blocked with PBS + 0.2% Triton, containing 2% of BSA for 45 min. Then, cells were incubated with the corresponding primary antibodies diluted in PBS plus 0.2% (v/v) Triton-2 % (w/v) BSA overnight at 4 ºC (Table 3). The next day, cells were washed with PBS 1X three times for 5 min. each and incubated with matching secondary antibodies conjugated with fluorophores diluted in PBS + 0.2% Tween for 1 h at room temperature (Table 3).

Click-iT EdU (5-ethynyl-2'-deoxyuridine) Proliferation Assay

Cells were fixed with 100% methanol at -20ºC and were labelled for Edu using the Click-iT EdU Alexa Fluor 488 HCS Assay according to manufacturer's instructions and co-stained with insulin. Cells were imaged using a Nikon spinning disk microscope at x20 magnification and counted using ImageJ software. At least 1000 cells were counted per experiment.

3-(4,5-Dimethylthiazol-2-yl)-2,5-diphenyltetrazolium bromide (MTT) assay.

The Cell Proliferation Kit I (MTT) (11465007001, Roche) assay was performed according to the manufacturer´s protocol. Briefly, Control and *PAX6-AS1* null cells were incubated with 0.5% MTT for 30 minutes. Then, blue formazan crystals were solubilized overnight with 100 µl of solubilization solution. Optical density was determined at 550 nm with a reference wavelength of 650 nm, using a Varioskan Flash spectrophotometer (Thermo Scientific).

Cell viability

Control and *PAX6-AS1* null cells were cultured for 30 min. in 1 ml of PBS with Calcein-AM (1 µl) (Molecular Probes, Eugene, OR) and propidium iodide (1 µl) (SigmaAldrich, St Louis, MO, USA). At least 1000 cells were counted for each experiment. Cells were imaged using a Nikon spinning disk microscope at x20 magnification and counted using ImageJ software. At least 1000 cells were counted per experiment.

Intracellular free [Ca^{2+}] measurements

Groups of 15 islets were incubated with the Ca^{2+} indicator Cal-520 (Abcam, ab171868) in KRBH supplemented with 3 mM glucose for 45 min. Islets were imaged using a Zeiss Axiovert microscope equipped with a ×10 0.3–0.5 NA objective at 3mM, 17mM and 20 mM KCl. Images were analysed using ImageJ software. Fluorescence intensity was normalised to basal glucose concentration (3mM) (F/F_{min}).

Immunoblotting

Cells were lysed in radioimmunoprecipitation assay buffer (RIPA buffer: 20 mM Tris-HCl, 50 mM NaCl, 1 mM Na_2-EDTA, 1 mM EGTA, 1% NP-40, 1% sodium deoxycholate) with 1% Phosphatase Inhibitor Cocktails (P0044 and P5725, Sigma-Aldrich) and 1% Protease Inhibitor

Cocktail (P8340, Sigma-Aldrich). Protein concentration was measured using a Pierce BCA Protein Assay Kit (Thermofisher, 23225) at 562 nm using a PHERAstar reader (BMG Labtech). After protein transfer to a polyvinylidene Difluoride (PVDF) membrane (Millipore), membranes were blocked with Tris-buffered saline 1X plus 0.1% (v/v/) Tween (TBST), containing 4% (w/v) BSA for 1h. Primary antibody incubation was performed overnight during rotation at 4 ºC in TBST-4% (w/v)BSA and horseradish peroxidase (HRP)-conjugated secondary antibody incubation was subsequently performed for 1 h in TBST-4% (w/v) milk powder (Table 2). Development usedClarity Western ECL Substrate (Bio-rad).

qRT-PCR

Total RNA was extracted using TRIZOL (Invitrogen, 15596026) following the manufacturer's instructions. Complementary DNA (cDNA) was synthesized using random primers (Roche) and the High-Capacity cDNA Reverse Transcription kit (Life Technologies). Real-time qPCR was performed with a SYBR Green PCR master mix (Applied Biosystems). Primers used in this study are outlined in table 4.

Luciferase reporter assay

Control and *PAX6-AS1*-depleted cells were co-transfected with pGL410_INS421 (Addgene #49057) and a renilla-encoding pRL-CMV vector. Cell extracts were collected 48 h post-transfection, and Dual-Luciferase Reporter Assay (Promega) was performed according to the manufacturer's instructions. The ratio between the luciferase and Renilla activities was expressed relative to the ratio obtained in control cells.

Subcellular fractionation

MIN6 cells were lysed using 200 µl lysis buffer (10 mM NaCl, 2 mM MgCl, 10mM Hepes, 5mM dithiothreitol (DTT), 0.5% Igepal CA 630 (Sigma I3021)) and placed on ice for 5 minutes. Centrifugation was performed at 8000 rpm, 4ºC for 5 min. The supernatant was collected as the cytoplasmic fraction while the pellet was resuspended in 200 µl lysis buffer to yield the nuclear fraction. Then, 200 µl of 2X ProtK buffer (0.2M Hepes, 25mM EDTA, 0.3M NaCl, 2% SDS) with 0.5U/µl RiboLock RNase inhibitor (Thermo fisher) were added. RNA was extracted from the independent fractions using TRizol reagent.

RNA pulldown assay

Pax6os1 or *Slc16a1* (control) were cloned using Sequence- and Ligation-Independent Cloning (SLIC) into a ptRNA-S1 plasmid that harbours a T7 promoter, *tRNA-S1 (encoding the streptavidin aptamer)* and a bovine growth hormone (BGH) polyadenylation site. Primers for *Pax6os1* amplification are described in table 3. The RNA input was prepared using 100 µg RNA, 1 U/µl RiboLock RNase inhibitor (ThermoFisher), and 1X Complete Proteinase inhibitor (Roche), in 1X Aptamer buffer (20 mM Hepes, 150 mM NaCl,10 mM $MgCl^2$, 0.5% (v/v) Triton X100, pH 7.02) and incubated with streptavidin beads (Sigma, S1638) at 4^{o}C for 4 h. Cellular extracts were prepared from MIN6 cells cultured in DMEM for SILAC without L-Arginine and L-Lysine (ThermoFisher, 88364) supplemented with 15% (v/v) FBS and either the light (R0 L-arginine, 12C6, (Sigma, A6969), K0 L-Lysine,12C6, (Sigma, L8662)) or heavy (R10 L-arginine-HCl, U-13C6, 15N4 (Cambridge isotope Lab. Cat no. CNLM-539), K8 L-Lysine - 2HCL, U-13C6, 15N4 (Cambridge isotope Lab. Cat no. CNLM-291)) isotypes. Two different SILAC MIN6 lysates were used with *Pax6os1* and *MCT1/SLC16A1* labelled with the heavy and light isotypes, respectively. Protein MIN6lysates (4 mg) were prepared by addition of Avidin (10 µg/mg protein) (Pierce, 21121) and yeast RNA (0.5 mg/mg protein) (Sigma, R6760) and supplemented with 1 U/µl RiboLock RNase inhibitor prior to being added to the streptavidin beads and incubated at 4^{o}C overnight under rotation. After 3 washes in 1X Aptamer buffer and one in 1X High salt aptamer buffer (20 mM Hepes, 400 mM NaCl, 10 mM $MgCl^2$, 0.5% (v/v) Triton X100), the streptavidin aptamer and bound complex were eluted using 50 µl 10 mM Biotin (pH 7.2) (Sigma, B4501) suspended in the 1X Aptamer buffer and stored at -20^{o}C.

Mass Spectrometry

The pooled SILAC samples were run into an SDS-PAGE gel and each gel lane cut into three slices. Each slice was subjected to in-gel tryptic digestion using a DigestPro automated digestion unit (Intavis Ltd.) and the resulting peptides were fractionated using an Ultimate 3000 nano-LC system in line with an Orbitrap Fusion Tribrid mass spectrometer (Thermo Scientific). In brief, peptides in 1% (vol/vol) formic acid were injected onto an Acclaim PepMap C18 nano-trap column (Thermo Scientific). After washing with 0.5% (vol/vol) acetonitrile 0.1% (vol/vol) formic acid peptides were resolved on a 250 mm × 75 µm Acclaim PepMap C18 reverse phase analytical column (Thermo Scientific) over a 150 min organic gradient, using 7 gradient segments (1-6% solvent B over 1min., 6-15% B over 58min., 15-32%B over 58min., 32-40%B

over 5min., 40-90%B over 1min., held at 90%B for 6min and then reduced to 1%B over 1min.) with a flow rate of 300 nl min−1. Solvent A was 0.1% formic acid and Solvent B was aqueous 80% acetonitrile in 0.1% formic acid. Peptides were ionized by nano-electrospray ionization at 2.0 kV using a stainless-steel emitter with an internal diameter of 30 μm (Thermo Scientific) and a capillary temperature of 275°C.

All spectra were acquired using an Orbitrap Fusion Tribrid mass spectrometer controlled by Xcalibur 3.0 software (Thermo Scientific) and operated in data-dependent acquisition mode. FTMS1 spectra were collected at a resolution of 120 000 over a scan range (m/z) of 350-1550, with an automatic gain control (AGC) target of 300 000 and a max injection time of 100ms. The Data Dependent mode was set to Cycle Time with 3s between master scans. Precursors were filtered according to charge state (to include charge states 2-6) and with monoisotopic peak determination set to Peptide. Previously interrogated precursors were excluded using a dynamic window (40s +/-10ppm). The MS2 precursors were isolated with a quadrupole mass filter set to a width of 1.4m/z. ITMS2 spectra were collected with an AGC target of 20 000, max injection time of 40ms and CID collision energy of 35%.

Secondary structure prediction

Secondary structure prediction was performed using RNAfold from the Viena package and visualized using VienaRNA webservices as well as R-chie webserver[28,29].

Statistical analysis

For comparisons between two groups, statistical significance was calculated using non-paired two-tailed Student's t-tests. For comparisons between more than two groups, one-way ANOVA or two-way ANOVA tests were performed. For metabolic tests, repeated measurements two-way ANOVA tests were performed. All the statistical analyses were performed using Graph Pad Prism 8.0. In all cases, a p-value < 0.05 was considered statistically significant. Error bars represent the standard error of the mean (SEM). Fluorescence intensity and images analyses were performed using ImageJ software.

Results

Pax6os1/*PAX6-AS1* expression is enriched in pancreatic islets and is upregulated in type 2 diabetes.

The lncRNA *Pax6os1*/*PAX6-AS1* is a 1,464/1,656 nucleotide transcript mapped in a syntenically conserved region in chromosome 2 in mice and chromosome 11 in humans. It is transcribed antisense to the *Pax6* gene, overlapping with intron 1 in both species. The first intron of *Pax6os1*/*PAX6-AS1* also overlaps with *Paupar*, another lncRNA that is mainly expressed in α-cells and it is involved in Pax6 splicing[21]. Nevertheless, *Pax6os1* is not highly conserved between species at the nucleotide level, containing 4 exons in mice and 3 in humans, and predicted secondary structures are different between species (Figure 1A and Supplemental Figure 1). Assessed across multiple mouse tissues by qRT-PCR analysis, *Pax6os1* tissue distribution was similar to that of *Pax6*, being predominantly expressed in pancreatic islets and to a lesser extent in the eye and brain (Figure 1B).

To determine whether *Pax6os1*/*PAX6-AS1* expression is modulated under conditions of glucotoxicity, mRNA levels of the lncRNA were measured at different glucose concentrations in both murine and human cell lines as well as primary islets. Interestingly, culture for 48 h in the presence of high glucose induced *Pax6os1* expression in MIN6 (15 and 35 vs 5 mM) (n=5. p= 0.02 and 0.03, respectively) and CD1 mouse-derived islets (11 vs 3 mM) (n=3, p<0.01) (Figure 1C-D). Furthermore, *Pax6os1* expression was increased in pancreatic islets from mice fed with HFD compared to control (n=6-5, p= 0.003), while *Pax6* mRNA levels remained unaffected (Figure 1E). Likewise, *PAX6-AS1* expression was upregulated in the human Endoc-βH1 cell line (n=5, p=0.01) as well as in human pancreatic islets (n=7, p= 0.03) cultured at elevated glucose concentrations (Figure 1F-G). Moreover, expression of *PAX6-AS1* was increased substantially (4-5fold) in islets from donors with type 2 diabetes versus normoglycemic donors (n=11-5, p-value<0.01, Figure 1H). In contrast, *Pax6* mRNA levels in islets from type 2 diabetes donors were not altered (Figure 1H).

Pax6os1 silencing upregulates β-cell signature genes in MIN6 cells

In order to study the effect of lowering *Pax6os1* in β-cells, we first transfected murine MIN6 cells with a small interfering RNA (siRNA) targeting the lnc-RNA. RNA-seq data showed that *Pax6os1* silencing ("knockdown"; KD) in MIN6 cells upregulated the expression of several β-cell signature genes, including *Ins2, Slc2a2, Pax6, Pdx1* and *Gck*, while further down-regulating several "disallowed genes" such as *Neurod1* and *Ldha* (Figure 2A). In addition,

insulin secretion and pathways associated with T2D were enriched after *Pax6os1* silencing in MIN6 cells (Figure 2B). qRT-PCR analyses cells confirmed a 35±5 % decrease in *Pax6os1* expression (p= 0.0005) as well as an increase in *Pax6* (1.28 ± 0.046 fold change; p= 005), *Glut2*/*Slc2a2* (1.52 ± 0.15 fold change; p= 0.0144) and *Mafa* (1.72 ± 0.31 fold change; p=0.040) mRNA levels (Figure 2C). However, despite the upregulation of several β-cell signature genes, β-cell functionality, as determined by glucose-stimulated insulin secretion (GSIS) assays, was not affected by *Pax6os1* silencing in MIN6 cells (Figure 2D-E).

Impact of *Pax6os1* deletion on glucose homeostasis in the mouse

In order to explore the possible consequences for insulin secretion and glucose homeostasis i*n vivo*, we used CRISPR/Cas9 gene editing to delete *Pax6os1* exon 1 plus the immediate 5' flanking region in the mouse. Analysis of Super-Low Input Carrier- Cap analysis of gene expression (SLIC-CAGE) data (NH, NC, BL, AMS, unpublished) in mouse islets identified independent transcription start sites (TSS) for *Pax6* and *Pax6os1*, located ~1kb apart (Supplemental Figure 2). Thus, the deletion generated only spanned *Pax6os1* TSS and its putative promoter, as suggested by the presence of accessible chromatin in this region (ATAC-seq data, unpublished results), and of H3K4me3[30] and H3K27Ac[31] chromatin marks (Supplemental Figure 2). However, whereas *Pax6os1* expression was lowered by > 95 % in islets from KO mice, *Pax6* mRNA levels were unaffected (Figure 3A-B).

No statistically significant differences were observed *in vivo* between wild-type (WT) and *Pax6os1* knockout (KO) male mice in weight (Figure 3C), glucose clearance (Figure 3E) or insulin secretion (Figure 3G) under standard (STD) diet at 8-9 weeks of age. Likewise, insulin secretion *in vitro* and glucose-stimulated Ca^{2+} dynamics were not significantly different between pancreatic islets from knockout and wild-type male mice under STD (Supplemental Figure 3A-D). Under HFD, *Pax6os1* KO male mice displayed normal weight gain, glucose tolerance and insulin secretion *in vivo* (Supplemental Figure 4A,C,E). In contrast, islets derived from *Pax6os1 KO* mice under HFD showed enhanced GSIS (n=9-5, p=0.04), while no effect was observed in calcium dynamics in response to glucose (Supplemental Figure 5A-B and E-F). Interestingly, *Pax6os1* KO female mice showed a tendency towards lowered body weight on both STD (Figure 3D) and HFD (Supplemental Figure 3B). However, no differences were observed in female *Pax6os1* KO mice under STD diet in glucose clearance (Figure 3F), insulin secretion *in vivo* and *in vitro* (Figure 3H and Supplemental Figure E-F) or glucose-stimulated Ca^{2+} dynamics (supplemental Figure G-H). In contrast, female *Pax6os1* KO mice on HFD

showed a tendency towards enhanced glucose clearance as determined by a lower peak at 30 minutes after the glucose load (p=0.041) and the AUC during an IPGTT performed at 12 weeks of age (8 weeks on HFD) (WT: 1212±169 a.u. vs *Pax6os1* KO: 1030±134 a.u p=0.069). However, these differences were not accompanied by enhanced insulin secretion or calcium dynamics in response to glucose (Supplemental Figure 4E-F and Supplemental figure 5C-D and G-H).

RNASeq analysis in islets from female mice aged 22 weeks maintained on regular diet revealed only minor changes. With the exception of *Pax6os1* (fold change=0.0108, p<0.0001, adjusted p-value: p=2.67E-16), only two genes (*Tnc*, an extracellular matrix protein[20], fold change=0.412, adjusted p-value: p=2.3E-6) and *Slc28a2*, a sodium nucleoside transporter[20], fold change=1.96, adjusted p-value: p=0.0518) showing dysregulated expression after correction for multiple testing. Nominally significant changes were seen for *Glut2/Slc2a2* (increased, uncorrected p-value p<0.01) and acyl-CoA thioesteerase-7 (*Acot7;* decreased, uncorrected p-value p<0.05), (Supplemental Figure 6). Tendencies were seen towards increases in the β-cell-enriched genes *G6pc2*, *Znt8/Slc30a8* and *Gipr*, and for a lowering of *Ghrl* expression, although *Pax6* expression was not affected (Supplemental Figure 6). This was reinforced by Gene Set Enrichment Analysis (GSEA) revealing that 'Pancreas Beta Cells' was the second most upregulated gene set as assessed by Normalised Enrichment Score (Supplemental Figure 6).

PAX6-AS1 knockout in EndoC-βH1 cells increases insulin content without affecting cell proliferation or viability

In order to determine the effect of *PAX6-AS1* knockout in adult human β-cells, we used a tailored CRISPR/Cas9 approach to delete ~80 bp within the first exon of *PAX6-AS1* in EndoC-βH1 cells (Supplemental Figure 2). We generated two different populations of EndoC-βH1 cells that exhibited a 47±6 % (n=6, p < 0.0001) decrease in *PAX6-AS1* expression. Remarkably, *PAX6-AS1* knockout (KO) EndoC-βH1 cells exhibited increased mRNAs levels of *PAX6* (1.60 ± 0.16 fold change, p= 0.002), *INS* (3.31 ± 0.62 fold change, p= 0.01), *SLC2A2* (1.74 ± 0.19 fold change, p= 0.003) and *MAFA* (2.26 ± 0.40 fold change, p= 0.01). In contrast, several genes characteristic of other endocrine cell lineages, such as *GHRL* (0.70 ± 0.09 fold change, p= 0.01) and *NEUROG3* (0.58 ± 0.02 fold change, p< 0.0001) were down-regulated in *PAX6-AS1* null compared to control cells (Figure 5A). We did not observe significant differences between genotypes in *PAX6* expression at the protein level as determined by Western (immuno-) blot

and immunofluorescence (Figure 4B-E). In contrast, *PAX6-AS1* deletion increased insulin protein levels, as determined by immunofluorescence, as well as by total insulin content (Control: 2125 ± 491 ng/ml vs *PAX6-AS1* KO: 3055 ± 691 ng/ml, p = 0.02) without affecting the proportion of insulin secreted in response to 17 vs 0.5 mM glucose (Figure 4D-H).

Interestingly, β-cell proliferation as determined by 5-ethynyl-2'-deoxyuridine (EdU) staining was not affected in *PAX6-AS1* null cells compared to controls (Figure 4I-J), but they exhibited increased oxidative metabolism as determined by a 3-(4,5-Dimethylthiazol-2-yl)-2,5-diphenyltetrazolium bromide (MTT) assay (125.3 ± 9.11%, p= 0.02) (Figure 5K). Since increased insulin content and oxidative metabolism can lead to endoplasmic reticulum (ER) stress and apoptosis, we next measured C/EBP-Homologous Protein 10/ DNA-Damage-Inducible Transcript 3 (*CHOP/DDIT3*) expression. No differences were observed between *PAX6-AS1* null and control cells in CHOP protein levels (Figure 4L-M). Likewise, *PAX6-AS1* KO cells did not exhibit increased apoptosis compared to control as determined by the percentage of calcein (live) and propidium iodide (apoptotic) positive cells (Figure 4N-O).

PAX6-AS1 knockdown enhances GSIS from human islets

In order to extend our results to fully differentiated human β-cells, we used lentiviral shRNA vectors to silence *PAX6-AS1* in pancreatic islets from post-mortem donors. Consistent with the results obtained in EndoC-βH1 cells, a reduction in *PAX6-AS1* expression of 49 ± 12%, upregulated *INS* mRNA levels (3.26 ± 1.05 fold change, p= 0.04), while *GHR* was downregulated (0.57 ± 0.05 fold change, p< 0.0001) and a small tendency towards increased *GLUT2/SLC2A2* expression was observed (Figure 6A). However, no significant differences were observed in the expression of other β-cell signature genes such as *PAX6* or *MAFA* (Figure 6A). More importantly, *PAX6-AS1* knockdown in human islets enhanced GSIS (Scrambled: 3.44 ± 0.74 fold change vs *PAX6-AS1* shRNA: 6.69 ± 1.78 fold change, p= 0.03) while total insulin content was not affected (Figure 5B-C). This finding was reinforced by the increased intracellular calcium dynamics in response to 17 mM glucose in *PAX6-AS1* knockdown islets assessed as the AUC for mean fluorescence (Scrambled: 805 ± 15.6 a.u. vs *PAX6-AS1* shRNA: 829 ± 11.3 a.u., p= 0.04) (Figure 5D-F). Responses to depolarisation with KCl were not significantly affected by *PAX6-AS1* silencing.

Pax6os1/PAX6-AS1 is located in both the cytoplasm and nucleus.

LncRNAs may regulate gene expression through a number of different mechanisms. These include chromatin remodelling, activation/repression of transcription factors in the nucleus as well as modulation of mRNA/protein stability in the cytoplasm[32,33]. Therefore, the subcellular localization of a lncRNA may provide a reliable indicator of its mechanism(s) of action. Determinations of *Pax6os1* subcellular localization in MIN6 cells (Methods) indicated that this lncRNA was located in both the nucleus (~40%) as well as in the cytoplasm (~60%) (Figure 6A).

Consistent with the above subcellular fractionation results, both nuclear and cytoplasmic proteins were identified by mass spectrometry as binding protein partners of *Pax6os1*. Interestingly, the top 5 hits included: Ras-related protein Rab8a, Eukaryotic translation initiation factor 3 subunit D (Eif3d), Inosine-5'-monophosphate dehydrogenase 2 (Impdh2), Short/branched chain-specific acyl-CoA dehydrogenase (Acadsb) and Histone 1.0 (Figure 6B-C). Therefore, our results suggest that *Pax6os1* may regulate the expression of target genes through a number of mechanisms, including chromatin remodelling (Histone 1.0) and RNA translation and stability (Eif3d). These actions may involve a number of different interacting proteins in both the nucleus and the cytoplasm.

DISCUSSION

Identifying the genetic networks that regulate β-cell differentiation and function is essential to understand the pathogenesis of type 2 diabetes and to find novel therapies to treat this disease. In recent years, several studies have shown the importance of long non-coding RNAs in the maintenance of β-cell identity[20,34].

In the present study, we show that *Pax6os1*/*PAX6-AS1*, a lncRNA transcribed from the *Pax6* locus and previously identified in the murine retina[22], is chiefly expressed in pancreatic islets. Importantly, our results show that the expression of this lncRNA is upregulated in an animal model of type 2 diabetes (high fat diet) as well as in pancreatic islets from patients with this disease, suggesting that increased expression of *PAX6-AS1* may contribute to the pathogenesis of T2D.

Although *Pax6os1* silencing increases the expression of several β-cell signature genes in MIN6 cells, indicating a role for the lncRNA in β-cell identity, we did not observe differences in functional assays *in vitro*. Similar to our findings in MIN6 cells, *PAX6-AS1* silencing in human

EndoC-βH1 cells, upregulated the expression of insulin and other β-cell signature genes without affecting glucose stimulated insulin secretion. In contrast, *PAX6-AS1* silencing in human pancreatic islets not only increased insulin mRNA levels but also enhanced glucose stimulated insulin secretion. Importantly, differences between immortalised and fully differentiated cells might also suggest a different role for *Pax6os1*/*PAX6AS1* at different stages of development/differentiation. Nevertheless, it is also important to note that differences in the phenotype observed between immortalised cells and islets may be also caused by differences in the system used to downregulate *PAX6-AS1*, since the ShRNA used in human islets may only block the actions of *PAX6-AS1* in the cytoplasm and not in the nucleus.

Strikingly, and despite the clear-cut effects of *Pax6os1*/*PAX6AS1* deletion or silencing in mouse and human β cells *in vitro*, mice in which *Pax6os1* was deleted *in utero* displayed little evidence of a glycaemic phenotype, or defective insulin secretion. Nevertheless, tendencies were observed to increase the expression of β-cell-enriched genes (*Glut, G6pc2, Slc30a8, Gipr*) and to further lower the expression of β-cell disallowed genes (*Acot7*), suggestive of reinforced β-cell identity [31].

Dissecting the functions of different transcripts within complex loci such as this is inherently difficult due to the close proximity of the transcriptional start sites. In an effort to mitigate these problems, we have used complementary techniques (shRNA and CRISPR) here to lower the levels of *Pax6os1/AS*1. It is important to note that the DNA fragment deleted (720 bp) by CRISPR/Cas9 to generate the *Pax6os1* knockout mice, might interfere with a regulatory region of *Pax6*, affecting the expression of the transcription factor directly and providing an explanation for the differences observed in *Pax6* levels between the different systems, i.e. that the loss of an inhibitory action of *Pax6os1* on the expression of target genes, potentially including *Pax6.* Assessment of the open chromatin state (ATACSeq) and regulatory histone marks indicated that the deletion intron 1 of *Pax6os1* and the proximal promoter region might conceivably exert an effect on *Pax6* expression *in cis*. Nevertheless, we note that since *Pax6os1* deletion had no effect on *Pax6* mRNA levels in mouse islets any negative action on *Pax6* transcription due to loss of a *cis*-acting regulatory region must be exactly balanced by the loss of a positive action of *Pax6os1 in trans*.

A further possible explanation for our findings is that early developmental compensation occurs *in vivo*, through presently-undefined mechanisms, which result in the normalisation of the expression of insulin and other genes essential for normal function. Of note, differences in

gene expression were also observed between EndoC-βH1 and islets, indicating that PAX6-AS1 may exert different effects depending on the differentiated state of the cell. Alternatively, the different phenotypes observed in EndoC-βH1 cells and human islets may reflect the different strategies used to reduce PAX6-AS1 levels, since the shRNA is likely to act only on the cytosolic lncRNA, while CRISPR deletion will affect the expression of PAX6-AS1 in both the cytoplasm and the nucleus.

Finally, our data may also support the view that there are important species differences in the importance of *Pax6os1/PAX6AS1*. Thus, and despite several similarities observed between the mouse and human models, *PAX6-AS1* depletion in human β-cells generally exerted larger effects than in mouse cells – including regulation of *INS* gene expression. Consistent with these results, predicted secondary structures differed between *Pax6os1* and *PAX6-AS1* (Supplemental Figure 1).

Could be there a role for *Pax6os1*/PAX6AS1 in both the nucleus and the cytosol? Consistent with this possibility, our results indicate that *Pax6os1* may be a bi-compartmental lncRNA, being present in both the nucleus and cytoplasm. The subcellular localizations of other, previously characterized lncRNAs, such as *MALAT1*, have been shown to be modulated according to the mitotic state of the cell[35]. Therefore, it is possible that *Pax6os1* subcellular localization and function are modulated depending on the maturity of the cell. This could explain the differences observed between immortalised and fully differentiated pancreatic cells. According to the results obtained by mass spectrometry, *Pax6os1* may interact with both nuclear and cytosolic proteins, affecting gene expression by interacting with histones or playing a role in mRNA capping and synthesis. In this sense, *Pax6os1* could play a dual function, in a manner similar to that observed for other lncRNAs, including *PYCARD-AS1*[36].

LncRNAs have emerged in recent years as promising therapeutic targets. Indeed, different approaches, including antisense oligonucleotides and small molecule inhibitors are being used to target lncRNAS in several diseases, such as cancer[37]. In the present study, we have shown that targeting *PAX6-AS1* could be a promising approach to promote β-cell differentiation and improve glucose homeostasis in patients with T2D, although a more extensive study will be required to further decipher the mechanism of action of this lncRNA.

In conclusion, we describe important roles and potential downstream mechanisms of action for a previously uncharacterised lncRNA in pancreatic β-cell function. We demonstrate roles in

the mature mouse and human β-cell, and in the control of insulin and other critical genes expression.

Author contributions

L.L.N and R.C performed most of the experiments and analysed data. A.M-S contributed to experiments with human islets. G.P. prepared RNAseq libraries. R.C and T.J.P. designed the CRISPR/Cas9 strategy and performed analysis of RNA-seq. A M-S, N.H., N.C. and B. L. generated SLIC-CAGE and performed the analysis of ATAC-seq and histone marks in mouse islets. P.M, L.P, E.K, A.M.J.S and P.J provided human islets. I.L. assisted with *in vivo* work. L.L.N and G.A.R wrote the manuscript. R.C and A.M-S critically reviewed the manuscript. T.J.P and G.A.R. conceived and supervised the study.

Acknowledgments

G.A.R. was supported by a Wellcome Trust Senior Investigator (WT098424AIA) and Investigator (WT212625/Z/18/Z) Awards, and MRC Programme grant (MR/R022259/1,), Diabetes UK (BDA/15/0005275) grants. AMS was support by an MRC New Investigator Research Grant (MR/P023223/1). NC was the recipient of an EMBO Advanced Long Term Fellowship (EMBO aALTF 626-2018) and BL received grants from the Wellcome Trust (106954) and Medical Research Council UK (MC UP 1102/1). This project has received funding from the European Union's Horizon 2020 research and innovation programme via the Innovative Medicines Initiative 2 Joint Undertaking under grant agreement No 115881 (RHAPSODY) to G.A.R and P.M.

Conflict of Interest

GAR has received grant funding and consultancy fees from Les Laboratoires Servier and Sun Pharmaceuticals. The remaining authors declare no conflict of interest.

References

1. DeFronzo RA. Insulin resistance, lipotoxicity, type 2 diabetes and atherosclerosis: the missing links. The Claude Bernard Lecture 2009. *Diabetologia.* 2010;53(7):1270-1287.
2. Ahlqvist E, Storm P, Käräjämäki A, et al. Novel subgroups of adult-onset diabetes and their association with outcomes: a data-driven cluster analysis of six variables. *Lancet Diabetes Endocrinol.* 2018;6(5):361-369.
3. Del Guerra S, Lupi R, Marselli L, et al. Functional and molecular defects of pancreatic islets in human type 2 diabetes. *Diabetes.* 2005;54(3):727-735.
4. Rutter GA, Pullen TJ, Hodson DJ, Martinez-Sanchez A. Pancreatic β-cell identity, glucose sensing and the control of insulin secretion. *Biochem J.* 2015;466(2):203-218.
5. Pullen TJ, Huising MO, Rutter GA. Analysis of Purified Pancreatic Islet Beta and Alpha Cell Transcriptomes Reveals 11β-Hydroxysteroid Dehydrogenase (Hsd11b1) as a Novel Disallowed Gene. *Front Genet.* 2017;8:41.
6. Pullen TJ, Khan AM, Barton G, Butcher SA, Sun G, Rutter GA. Identification of genes selectively disallowed in the pancreatic islet. *Islets.* 2010;2(2):89-95.
7. Neelankal John A, Ram R, Jiang FX. RNA-Seq Analysis of Islets to Characterise the Dedifferentiation in Type 2 Diabetes Model Mice db/db. *Endocr Pathol.* 2018;29(3):207-221.
8. Moin ASM, Butler AE. Alterations in Beta Cell Identity in Type 1 and Type 2 Diabetes. *Curr Diab Rep.* 2019;19(9):83.
9. Ding J, Gao Y, Zhao J, et al. Pax6 haploinsufficiency causes abnormal metabolic homeostasis by down-regulating glucagon-like peptide 1 in mice. *Endocrinology.* 2009;150(5):2136-2144.
10. Liu T, Zhao Y, Tang N, et al. Pax6 directly down-regulates Pcsk1n expression thereby regulating PC1/3 dependent proinsulin processing. *PLoS One.* 2012;7(10):e46934.
11. Swisa A, Avrahami D, Eden N, et al. PAX6 maintains β cell identity by repressing genes of alternative islet cell types. *J Clin Invest.* 2017;127(1):230-243.
12. Ashery-Padan R, Zhou X, Marquardt T, et al. Conditional inactivation of Pax6 in the pancreas causes early onset of diabetes. *Dev Biol.* 2004;269(2):479-488.
13. Mitchell RK, Nguyen-Tu MS, Chabosseau P, et al. The transcription factor Pax6 is required for pancreatic β cell identity, glucose-regulated ATP synthesis, and Ca2+ dynamics in adult mice. *J Biol Chem.* 2017;292(21):8892-8906.
14. Parton LE, McMillen PJ, Shen Y, et al. Limited role for SREBP-1c in defective glucose-induced insulin secretion from Zucker diabetic fatty rat islets: a functional and gene profiling analysis. *Am J Physiol Endocrinol Metab.* 2006;291(5):E982-994.
15. Wu H, Liu Y, Wang H, Xu X. High-fat diet induced insulin resistance in pregnant rats through pancreatic pax6 signaling pathway. *Int J Clin Exp Pathol.* 2015;8(5):5196-5202.
16. Yasuda T, Kajimoto Y, Fujitani Y, et al. PAX6 mutation as a genetic factor common to aniridia and glucose intolerance. *Diabetes.* 2002;51(1):224-230.
17. Nishi M, Sasahara M, Shono T, et al. A case of novel de novo paired box gene 6 (PAX6) mutation with early-onset diabetes mellitus and aniridia. *Diabet Med.* 2005;22(5):641-644.
18. Taneera J, Lang S, Sharma A, et al. A systems genetics approach identifies genes and pathways for type 2 diabetes in human islets. *Cell Metab.* 2012;16(1):122-134.

19. Singer RA, Sussel L. Islet Long Noncoding RNAs: A Playbook for Discovery and Characterization. *Diabetes.* 2018;67(8):1461-1470.
20. Morán I, Akerman I, van de Bunt M, et al. Human β cell transcriptome analysis uncovers lncRNAs that are tissue-specific, dynamically regulated, and abnormally expressed in type 2 diabetes. *Cell Metab.* 2012;16(4):435-448.
21. Singer RA, Arnes L, Cui Y, et al. The Long Noncoding RNA Paupar Modulates PAX6 Regulatory Activities to Promote Alpha Cell Development and Function. *Cell Metab.* 2019;30(6):1091-1106.e1098.
22. Alfano G, Vitiello C, Caccioppoli C, et al. Natural antisense transcripts associated with genes involved in eye development. *Hum Mol Genet.* 2005;14(7):913-923.
23. Jimenez-Moreno CM, Herrera-Gomez IG, Lopez-Noriega L, et al. A Simple High Efficiency Intra-Islet Transduction Protocol Using Lentiviral Vectors. *Curr Gene Ther.* 2015;15(4):436-446.
24. Kim D, Paggi JM, Park C, Bennett C, Salzberg SL. Graph-based genome alignment and genotyping with HISAT2 and HISAT-genotype. *Nat Biotechnol.* 2019;37(8):907-915.
25. Liao Y, Smyth GK, Shi W. featureCounts: an efficient general purpose program for assigning sequence reads to genomic features. *Bioinformatics.* 2014;30(7):923-930.
26. Love MI, Huber W, Anders S. Moderated estimation of fold change and dispersion for RNA-seq data with DESeq2. *Genome Biol.* 2014;15(12):550.
27. López-Noriega L, Cobo-Vuilleumier N, Narbona-Pérez Á, et al. Levothyroxine enhances glucose clearance and blunts the onset of experimental type 1 diabetes mellitus in mice. *Br J Pharmacol.* 2017;174(21):3795-3810.
28. Lai D, Proctor JR, Zhu JY, Meyer IM. R-CHIE: a web server and R package for visualizing RNA secondary structures. *Nucleic Acids Res.* 2012;40(12):e95.
29. Lorenz R, Bernhart SH, Höner Zu Siederdissen C, et al. ViennaRNA Package 2.0. *Algorithms Mol Biol.* 2011;6:26.
30. Lu TT, Heyne S, Dror E, et al. The Polycomb-Dependent Epigenome Controls β Cell Dysfunction, Dedifferentiation, and Diabetes. *Cell Metab.* 2018;27(6):1294-1308.e1297.
31. Nammo T, Udagawa H, Funahashi N, et al. Genome-wide profiling of histone H3K27 acetylation featured fatty acid signalling in pancreatic beta cells in diet-induced obesity in mice. *Diabetologia.* 2018;61(12):2608-2620.
32. Alessio E, Bonadio RS, Buson L, Chemello F, Cagnin S. A Single Cell but Many Different Transcripts: A Journey into the World of Long Non-Coding RNAs. *Int J Mol Sci.* 2020;21(1).
33. Wen X, Gao L, Guo X, et al. lncSLdb: a resource for long non-coding RNA subcellular localization. *Database (Oxford).* 2018;2018:1-6.
34. Akerman I, Tu Z, Beucher A, et al. Human Pancreatic β Cell lncRNAs Control Cell-Specific Regulatory Networks. *Cell Metab.* 2017;25(2):400-411.
35. Noh JH, Kim KM, McClusky WG, Abdelmohsen K, Gorospe M. Cytoplasmic functions of long noncoding RNAs. *Wiley Interdiscip Rev RNA.* 2018;9(3):e1471.
36. Miao H, Wang L, Zhan H, et al. A long noncoding RNA distributed in both nucleus and cytoplasm operates in the PYCARD-regulated apoptosis by coordinating the epigenetic and translational regulation. *PLoS Genet.* 2019;15(5):e1008144.
37. Mishra S, Verma SS, Rai V, et al. Long non-coding RNAs are emerging targets of phytochemicals for cancer and other chronic diseases. *Cell Mol Life Sci.* 2019;76(10):1947-1966.

38. Mularoni L, Ramos-Rodríguez M, Pasquali L. The Pancreatic Islet Regulome Browser. *Front Genet.* 2017;8:13.

Tables.

Table 1. List of donor characteristics and isolation centres.

Identifier	Sex	Age	BMI	Isolation Centre
49 (T2D)	Male	55	23.6	Edmonton, Canada (Macdonald)
60	Male	61	27.8	Milan
74	Male	83	24.5	Pisa
78 (T2D)	Female	54	30.8	Edmonton, Canada (McDonald)
80	Male	54	35	Edmonton, Canada (McDonald)
85	Female	62	23.9	Pisa
91 (T2D)	Female	53	21	Leiden
95	Male	38	42.6	Edmonton, Canada (McDonald)
101 (T2D)	Male	57	35	Leiden
106	Female	49	20.57	Milan
114	Female	46	35	Oxford
116	Female	55	26	Milan
127 (T2D)	Male	57	32	Oxford
165	Female	55	25	Oxford
177				Milan
178	Female	unvavailable	25.4	Pisa
182	Male	34	27	Oxford
188	Male	44	26	Oxford
189	Female	85	23.3	Pisa
190	Female	68	25.39	Pisa
193	Male	46	29.39	Pisa

Table 2. GuideRNAs used for CRISPR/Cas9 mediated disruption.

Human	Mouse
5’-CACCGGTCCGGCCGCACGCCTTACC-3’	CACCGTGGTGGCCACTTTGCCCG
5’-CACCGCAGGTCGCCTGCTTCGCAGT-3’	CACCGTTGTTTCCTCGGAGATCG

Table 3. Antibodies used in this study

Antibody	Dilution	Vendor	Catalog number
Anti-Pax6	1:1000 WB, 1:100 IF	Biolegend	PRB-278P
Anti-Insulin	No diluted	Dako	IR002
Anti-GADD153 (CHOP)	1:200	Santa Cruz Biotechnology	sc-575
Anti-GAPDH	1:2000	Cell Signaling	2118
488 Donkey anti-rabbit	1:500	Invitrogen	A21206
568 goat anti-guinea pig	1:500	Invitrogen	A11075
Goat Anti-Mouse (HRP)	1:5000	Abcam	ab6789
Goat Anti-Rabbit (HRP)	1:5000	Abcam	ab6721

Table 4. Primers used in this study.

Gene	Forward	Reverse
Pax6os1-202 (mouse)	AGATGCCTTAGACAAGCCTG	ATTCACCTTCTTGGACCCTG
Pax6os1-201 (mouse)	AGATGCCTTAGACAAGCCTG	ATTCACCTTCTTGGACCCTG
Pax6 (mouse)	ATGGGCGGAGTTATGATACCT	TGAAATGAGTCCTGTTGAAGTG
Beta Actin (mouse)	CGAGTCGCGTCCACCC	CATCCATGGCGAACTGGTG
Insulin 2 (mouse)	AGTAACCACCAGCCCTAAGTG	AGCACTGATCTACAATGCCAC
SLC2A2 (Glut 2) (mouse)	TTACAGTCACACCAGCATACAC	GCTTTGATCCTTCCAAGTTTGTC

Pdx1 (mouse)	GATGAAATCCACCAAAGCTC	TCGGTCAAGTTCAACATCAC
Foxa2 (mouse)	CCCATTCTGGACATGGTGAAA	AGCACGCAGAAACCATAAATTAAA
Arx (mouse)	CCGCTGGGTCTGAGCACTT	GAAAAGAGCCTGCCAAATGC
Pax4 (mouse)	ATCCAGAACCAGTCCCAAAGAG	CCAACTGGCAAACTGAAAACG
Mafa (mouse)	CAGGTGGAGCAGCTGAAGCT	CCGCCAACTTCTCGTATTTCTC
Mafb (mouse)	CGCGTCCAGCAGAAACATC	AGCTGCTCCACCTGCTGAAT
Ghrelin (mouse)	GCTGGAGATCAGGTTCAATGC	CTGCTGATACTGAGCTCCTGACA
Irx2 (mouse)	GAGGACGAAGGGATCAGTCTACA	CGGCAGGGCAATTTTTCC
Gapdh (mouse)	AGGTCGGTGTGAACGGATTTG	GGGGTCGTTGATGGCAACA
Ldha	ATGAAGGACTTGGCGGATGA	ATCTCGCCCTTGAGTTTGTCTT
RNA, U6 small nuclear 1 (RNU6-1) (mouse)	CGATACAGAGAAGATTAGCATGG	AATATGGAACGCTTCACGA
Gck (mouse)	CAACTGGACCAAGGGCTTCAA	TGTGGCCACCGTGTCATTC
PAX6-AS1 (human)	CAGCTCCAGGGAGAGGAAC	GAAGACACTCCTCCAGCAGAA
PAX6-AS1 (human)	AGCTGCTGCCTTTCTCAAAA	CATTACTGCTGAGGGCCTTG
INS (human)	GCAGCCTTTGTGAACCAACA	ACCTGCCCCACCTGCAG
PAX6 (human)	CCGTGTGCCTCAACCGTA	CACGGTTTACTGGGTCTGG
Cyclophilin (human)	TATCTGCACTGCCAAGACTGA	CCACAATGCTCATGCCTTCTTTCA

MAFA (human)	GCCATCGAGTACGTCAACGA	CGGGAGGCTCCTTCTTCAC
MAFB (human)	TTCTTTGGGTGAGAAGGGATCGCA	TCAGCTTGCTGCCACGTTCTCTAT
NEUROD1 (human)	ATTGCACCAGCCCTTCCTTTGATG	TCGCTGCAGGATAGTGCATGGTAA
NEUROG3 (human)	TAAGAGCGAGTTGGCACTGAGCAA	TTTGAGTCAGCGCCCAGATGTAGT
PDX1 (human)	TACTGGATTGGCGTTGTTTGTGGC	AGGGAGCCTTCCAATGTGTATGGT
SLC2A2 (human)	AGCTGCATTCAGCAATTGGACCTG	ATGTGAACAGGGTAAAGGCCAGGA
LDHA (human)	AGCCCGATTCCGTTACCT	CACCAGCAACATTCATTCCA
GHRL (human)	GGAAGATGGAGGTCAAGCAG	GCCTCTTCCCAGAGGATGTC

FIGURE LEGENDS.

Figure 1. *Pax6os1* is chiefly expressed in β-cells in the mouse and is upregulated by high fat diet as well as in islets from patients with type 2 diabetes. A) Schematic representation of the long non-coding RNA identified at the Pax6 locus in mice and humans. **B)** Tissue distribution of *Pax6os1* expression. n=3. **C, D)** *Pax6os1* and Pax6 expression in MIN6 cells and CD1 mouse pancreatic islets cultured at different glucose concentrations for 48h. MIN6cells: n=6. CD1 islets: n= 3. **E)** *Pax6os1* and Pax6 expression in pancreatic islets from C57/BL6 mice in standard (STD) or high fat diet (HFD) for 8 weeks. n=6. **F, G)** *PAX6-AS1* and PAX6 mRNA expression in EndoC-βH1 cells and human islets cultured with different glucose concentrations for 48 hs. EndoC-βH1 n=5. Human islets n=7. **H)** *PAX6-AS1* and PAX6 expression in human pancreatic islets from normoglycemic or diabetic donors. Control, n=10; Diabetic, n=5. Data are represented as the mean ± SEM. * p-value < 0.05 one-way ANOVA repeated measurements.

Figure 2. *Pax6os1* silencing upregulates β-cell signature genes in MIN6 cells. A) Differential expressed genes by *Pax6os1* knockdown as determined by RNA-seq performed in MIN6 cells 72 h post-transfection with s siRNA targeting *Pax6os1*. n= 4. **B)** KEGG pathway enrichment analysis relative to A. Significantly enriched KEGG pathways ($p < 0.05$) are presented and the bar shows the fold-enrichment of the pathway. **C)** mRNA levels of β-cell signature genes and markers characteristic of other endocrine cell lineages in control and *Pax6os1* knockdown cells. n= 7. **D)** Fold change of insulin secreted relative to 3mM glucose. **E)** Total insulin content per well. Data are represented as the mean ± SEM. *p-value< 0.05, student t-test.

Figure 3. *Pax6os1* knockout mice display normal glucose tolerance and insulin secretion compared to WT. **A, B)** *Pax6os1* and Pax6 expression in wt (+/+), *Pax6os1* heterozygous (+/-) and *Pax6os1* homozygous (-/-) mice. **C, D)** Body weights (g) of male and female mice, respectively. **E, F)** Circulating glucose levels during an intraperitoneal glucose tolerance test (IPGTT). **G, H)** Plasma insulin levels after an intraperitoneal glucose load (3g/kg). Data are represented as the mean ± SEM. *p-value < 0.05 Repeated measurements two-way ANOVA.

Figure 4. CRISPR/Cas9-mediated *PAX6-AS1* deletion from EndoC-βH1 cells increases insulin content without affecting cell number. A) mRNA expression of *PAX6-AS1*, β-cell signature genes and markers from other endocrine cell lineages in *PAX6-AS1* deleted EndoC-BH1 cells. *PAX6-AS1*, n= 6; *PAX6*, n= 6; *INS*, n= 4; *GLUT2/SLC2A2*, n= 5; *PDX1*, n= 4; *MAFB* n= 4; ARX, n= 3; GHRL, n= 4; NEUROG3, n= 3; NEUROD1, n= 5; LDHA, n=4. **B)** Western blot showing Pax6 protein levels. **C)** Densitometric analysis for B. **D)** Representative images of PAX6 and insulin fluorescence staining. Scale Bar: 100 µm. **E, F)** Quantification of PAX6 and insulin staining (mean intensity), respectively. n=3. **G)** Determination of total insulin content per well. n= 5. **H)** Fold change of glucose induced insulin secretion. n= 5. **I, J)** Proliferation in *PAX6-AS1* deleted EndoC-βH1 cells assessed by EdU staining: quantification (I, n = 5) and representative images (J). **K)** Oxidative phosphorylation as determined by an MTT assay in *PAX6-AS1* deleted EndoC-βH1 cells. n=5. **L)** Western (immuno-) blot showing CHOP expression in *PAX6-AS1* null EndoC-βH1 cells. **M)** Densitometric analysis of the

western blot shown in panel L. **N)** Representative images showing calcein (green) and propidium iodide (red) staining. **O)** Quantification of the percentage of propidium iodide positive cells. Data are represented as the mean ± SEM. * p-value< 0.05, Student's t-test.

Figure 5. ShRNA-mediated *PAX6-AS1* knockdown in human islets increases glucose-induced insulin secretion. Human islets were infected with a scrambled shRNA or a shRNA targeting *PAX6-AS1*. **A)** mRNA expression of *PAX6-AS1*, β-signature genes and markers from other endocrine cell lineages. n= 4-5. **B)** Determination of pancreatic islet insulin content. n= 5. **C)** Glucose induced insulin secretion represented as the fold change. n= 5. **D)** Representative images showing calcium response. **E, F)** Area under the curve (AUC) and trace showing calcium response in *PAX6-AS1* silenced islets. n= 4. Data are represented as mean ± SEM. * p-value < 0.05, student's t-test.

Figure 6. *Pax6os1* is located in the nucleus and cytoplasm and affects gene expression through several different mechanisms. A) Subcellular localisation of *Pax6os1*, Pax6, U6 (nuclear marker), *Gapdh* (cytosolic marker) and β-actin (*Actb*; cytosolic marker) expressed as a percentage of the total expression in both fractions. **B)** Relationship in abundance ratios of all hits obtained by mass spectrometry between the *Pax6os1* enrichment (green box) and control enriched (red box). **C)** Relationship in abundance ratios above the 1.1 cut between the two experimental replicates performed. Top 5 hits are labelled. Short/branched chain-specific acyl-CoA dehydrogenase, mitochondrial 1 (Acadsb), Eukaryotic translation initiation factor 3 subunit D (Eif3d), Inosine-5'-monophosphate dehydrogenase 2 (Impdh2), Histone 1.0 (H1.0), Uncharacterized protein Rab8a (Rab8a). Data are represented as the mean ± SEM. *p-value < 0.05, student's t-test.

Supplemental Figures.Supplemental Figure 1. *Pax6os1* and PAX6-AS1 secondary structure predictions. A) Secondary structure predicted using RNAfold from the VIENA package for *Pax6os1* and *PAX6-AS1*, respectively and drew using FORNA webserver. **B)** Comparison between the secondary structures predicted for *Pax6os1* (green) and *PAX6-AS1*(grey) represented as arch diagrams using R-chie webserver. Archs represent predicted base pairs.

Supplemental Figure 2. **Chromatin landscape of the Pax6os1 locus.** Integration of ATAC-seq displaying chromatin accessibility (yellow), SLIC-CAGE showing TSSs (Minus strand, red; Plus strand, green) and H3K4me3 (Lu et al., GEO: GSE110648) and H3K27Ac (Nammo et al, E-MTAB-6719) ChIP-seq datasets (blue) in mouse islets. Annotated (GENCODE VM23) of non-coding (Pax6os1 and Paupar) and coding transcripts including spliced variants (Pax6) are shown in blue, with arrows indicating transcription directionality. The region deleted in *Pax6os1* KO mice is shown in pale blue. Alignment with the human DNA track is shown at the bottom. **B)** Diagram showing deleted regions in and around *PAX6-AS1* in human β-cells and chromatin marks found in the *PAX6-AS1* and *PAX6* locus (obtained from the pancreatic islet regulome browser[38]). *PAX6-AS1* is annotated as DKFZp686K1684.

Supplemental Figure 3. *Pax6os1* KO mice display normal *in vitro* glucose-stimulated insulin secretion and Ca^{2+} dynamics. A, B) Percentage of insulin secreted relative to total content and fold change in pancreatic islets from male wt(+/+) and *Pax6os1*(-/-) mice *in vitro*. **C, D)** As in A and B but in females. **E, F)** Traces showing calcium dynamics represented as the fold change from basal glucose and AUC in islets isolated from male wt(+/+) and *Pax6os1*knockout (-/-) mice**. G, H)** As in E and F but in islets isolated from female mice. Data are represented as the mean ±SEM.**Supplemental Figure 4. *Pax6os1* female null mice display mildly improved glucose tolerance and normal insulin secretion compared to WT animals under HFD. A, B)** Body weights (g) of wt (+/+), *Pax6os1* heterozygous (+/-) and *Pax6os1* homozygous (-/-) male and female mice, respectively. **C, D)** Circulating glucose levels during an intraperitoneal glucose tolerance test (IPGTT). **E, F)** Plasma insulin levels after an intraperitoneal glucose load (3g/kg). Data are represented as the mean ± SEM. *p-value < 0.05 Repeated measurements two-way ANOVA.

Supplemental Figure 5. GSIS and Ca^{2+} dynamics in islets derived from *Pax6os1* null mice under HFD. A, B) Percentage of insulin secreted relative to total content and fold change in pancreatic islets from male wt(+/+) and *Pax6os1*(-/-) mice fed with HFD *in vitro*. **C, D)** As in A and B but in females. **E, F)** Traces showing calcium dynamics represented as the fold change from basal glucose and AUC in islets isolated from male wt(+/+) and *Pax6os1*knockout (-/-) mice fed with HFD**. G, H)** As in E and F but in islets isolated from female mice. Data are represented as the mean ±SEM. *p-value < 0.05, student's t-test.

Supplemental Figure 6. Expression changes for genes associated with β-cell identity following knockout of *Pax6os1* in mice. A) Genes are grouped and colour coded accordingly of their function. Data are presented as fold change in expression vs wild-type controls. A value of 1.0 signifies no change from the wild-type to the knockout and is marked by the black dotted line. n=4 per genotype (+/+; -/-). **B)** All genes with detectable expression were ranked by log-fold change and subjected to GSEA using MSigDB Hallmark pathways. The second most upregulated pathway as assessed by positive Normalised Enrichment Score was 'Pancreas Beta

Cells'. The GSEA plot along with the genes identified in the Leading Edge analysis are shown on the right. Unadjusted (nominal) p-values; *p<0.05, **p<0.01, ****p<0.0001

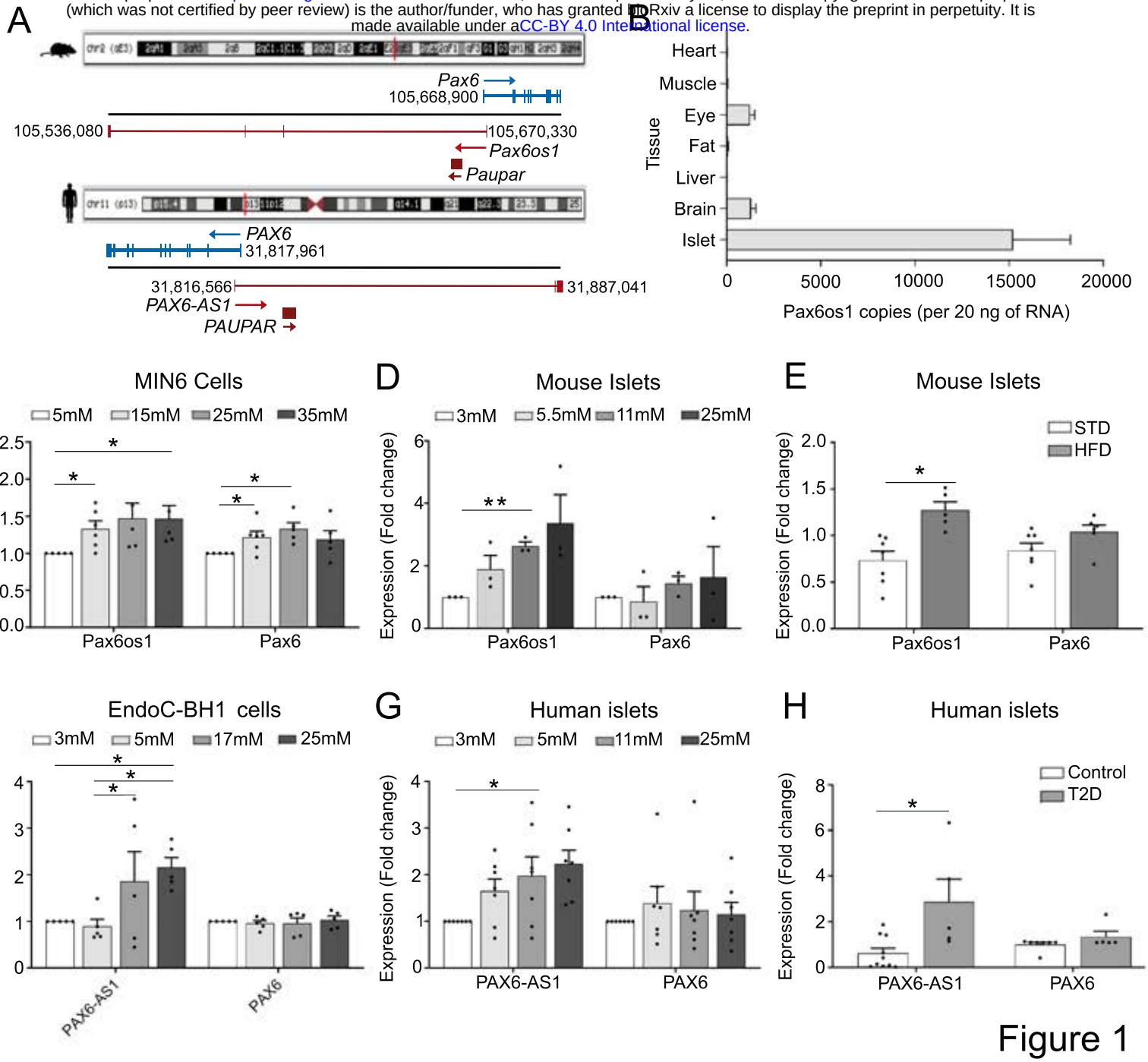

Figure 1

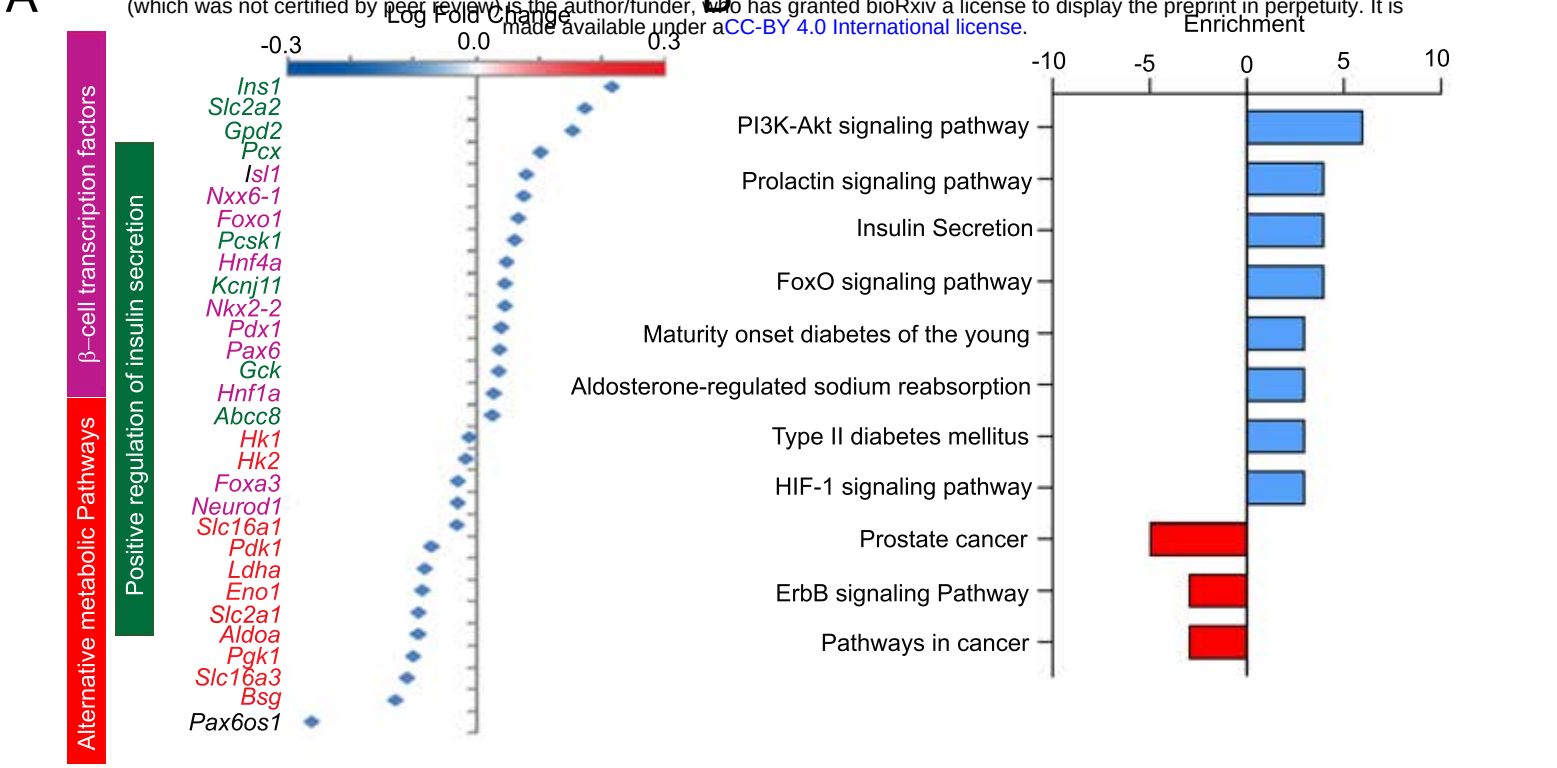

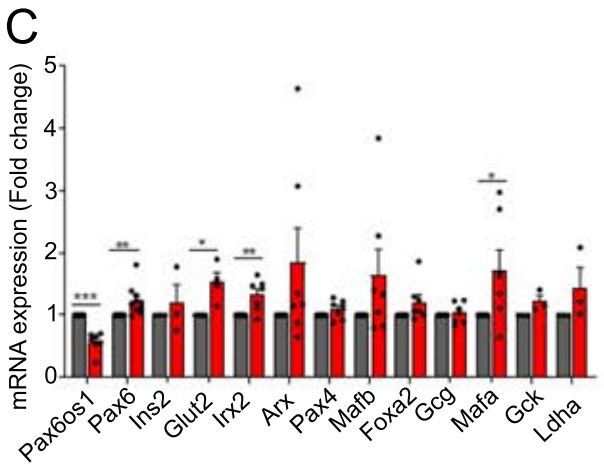

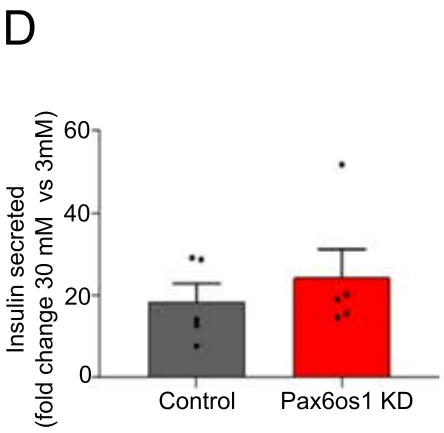

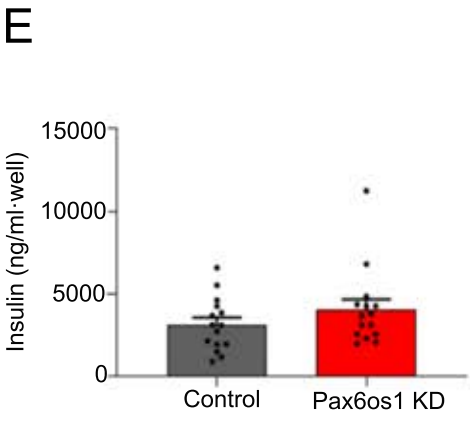

Figure 2

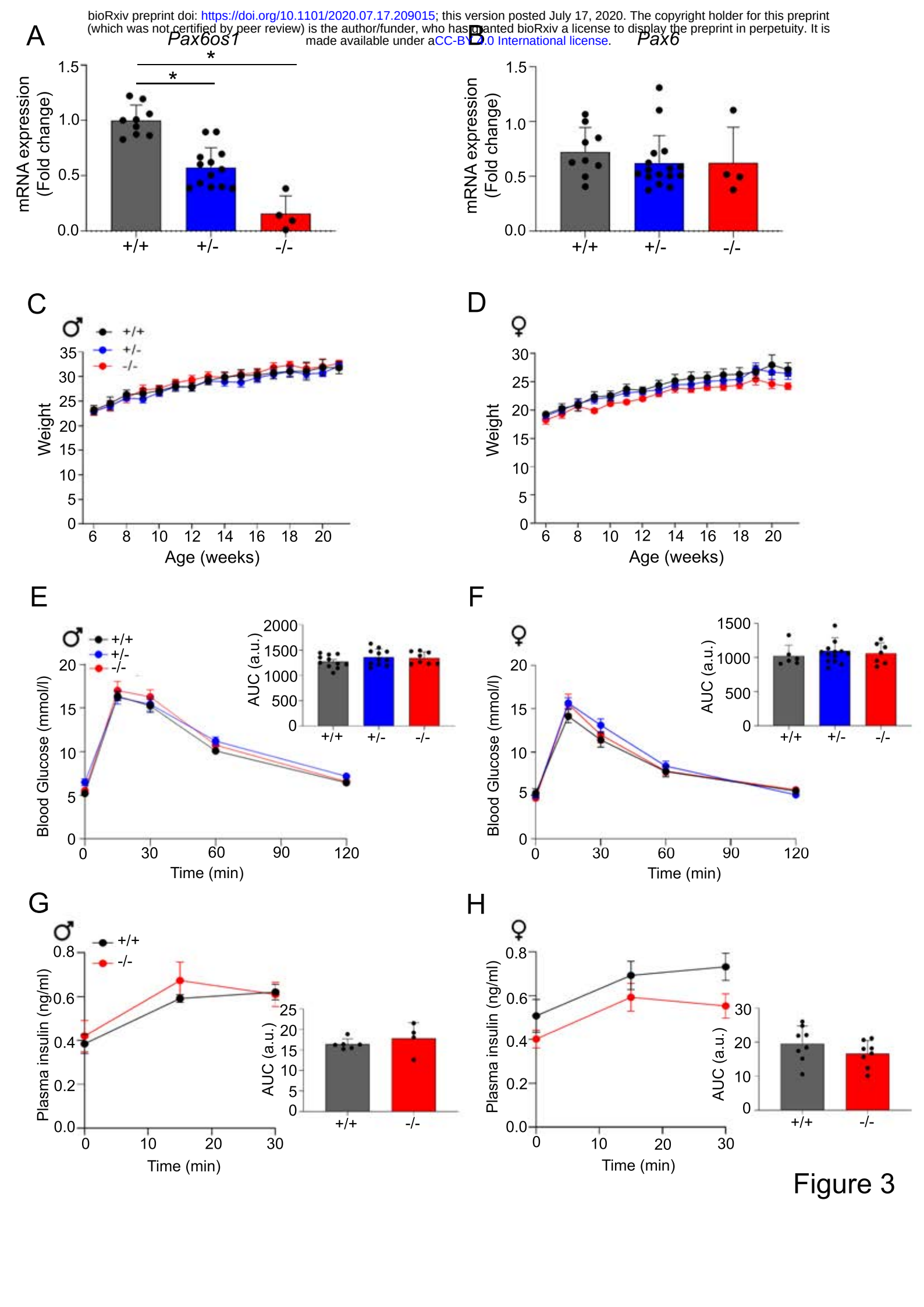

Figure 3

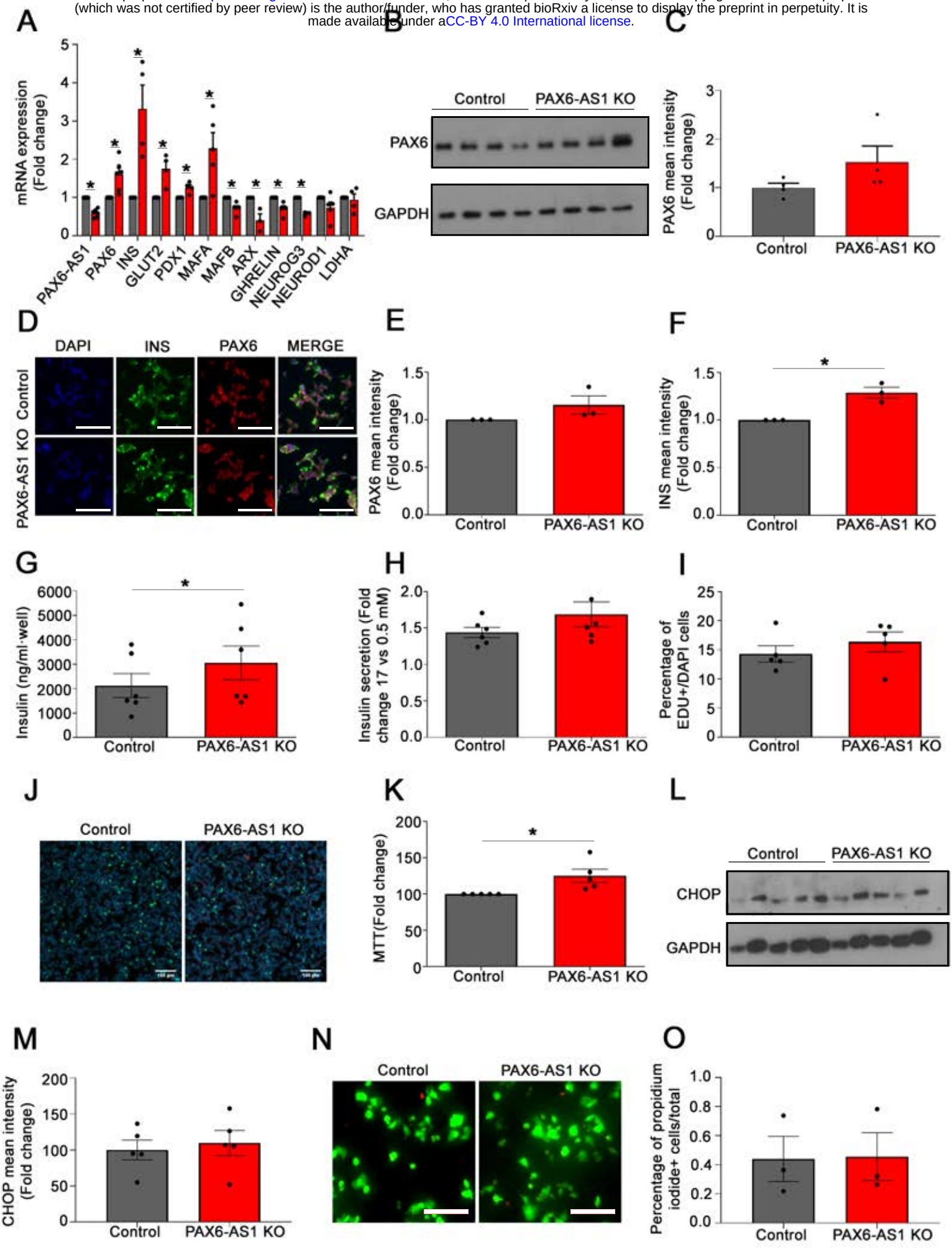

Figure 4

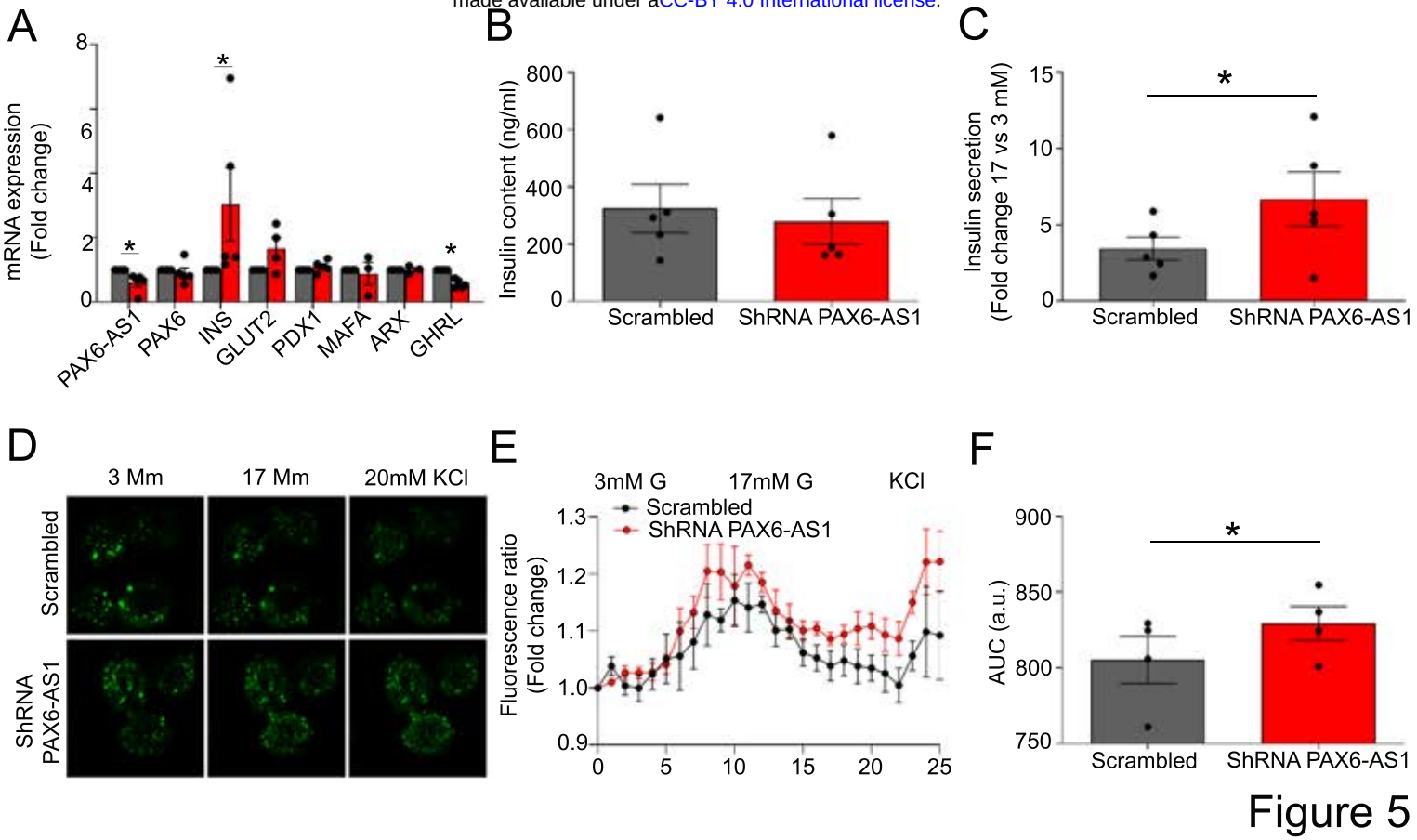

Figure 5

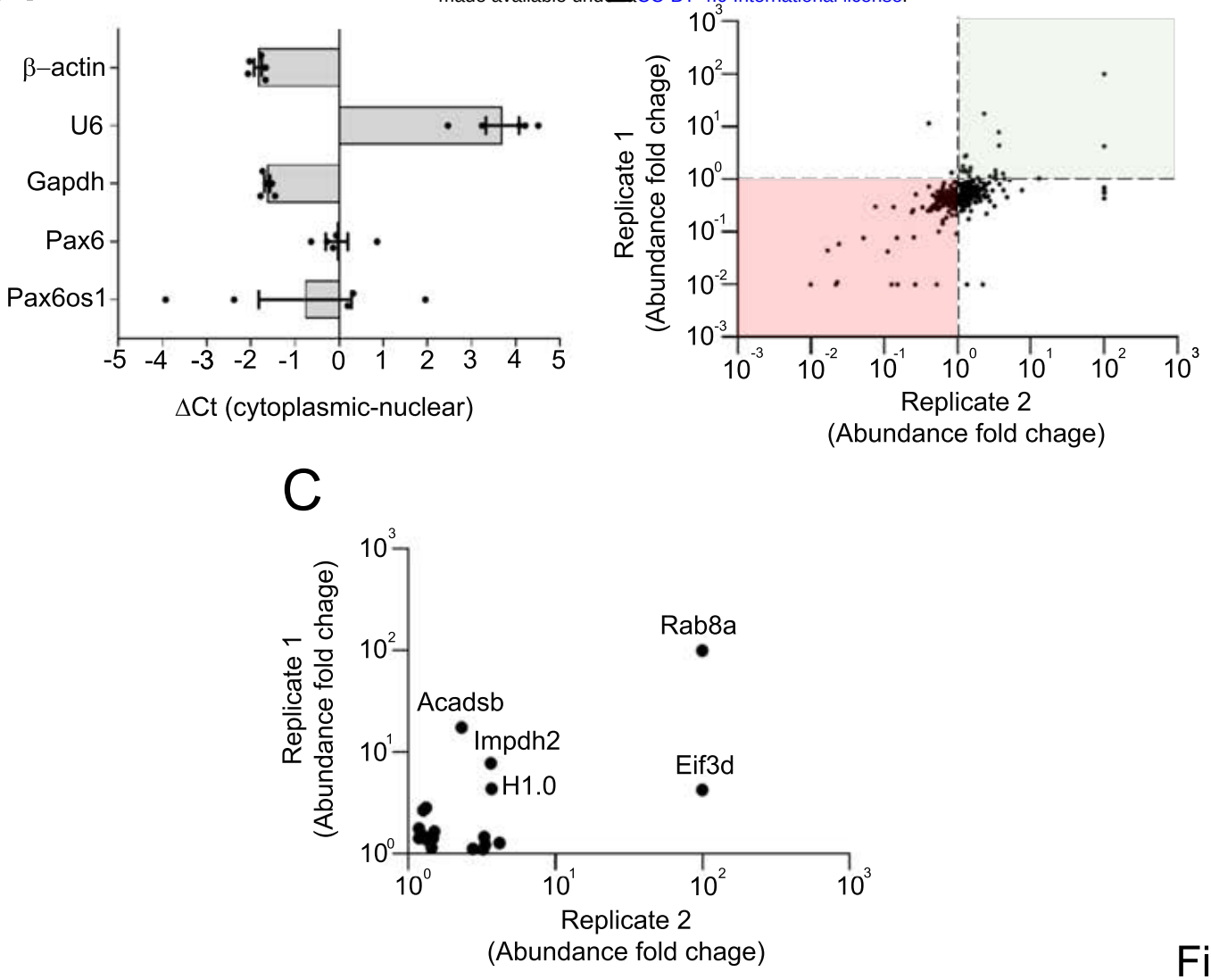

Figure 6